Ab Initio Studies of Silica-Based Clusters. Part II. Structures and Energies of Complex Clusters

J. C. G. Pereira,*,†,‡ C. R. A. Catlow,† and G. D. Price‡

The Royal Institution of Great Britain, 21 Albemarle Street, London W1 X 4BS, United Kingdom, and Department of Geological Sciences, University College London, Gower Street, London WC1E 6BT, United Kingdom

Received: July 2, 1998; In Final Form: November 18, 1998

We report density functional calculations on the energies and conformations of complex silica-based clusters, after our analysis of the simpler clusters reported in part I. We report calculated structures, charge distributions, and energies of the noncyclic four- and five-silicon chains, the branched trimer and tetramer rings, the double trimer rings, the tetramer plus trimer rings, the five- and six-silicon rings; all calculations are at the local density level of approximation. The total condensation energy (from the monomer) to form a silica cluster in the gas phase depends essentially on its structure and size. Our results show that the stability of the noncyclic clusters decreases with the degree of branching, as observed experimentally. This trend is observed for both four-silicon and five-silicon clusters. As expected, the double ring clusters are quite unstable, which is especially marked for the double trimer rings. Formation of trimer−tetramer rings is energetically more favorable, particularly for the edge-linked cluster. The four- and six-silicon rings are more stable than the corresponding pentamer because of the relatively asymmetric arrangement of the latter.

1. Introduction

As discussed in part I of this study,[1] knowledge of the structures, stabilities, and reactions of small silicate clusters is of crucial importance in developing an understanding of the molecular processes occurring in both sol−gel synthesis of ceramics and hydrothermal synthesis of microporous materials. The inorganic polymerization occurring in silica-based sol−gel processes results in the water and alcohol condensation of the silanol groups formed during the hydrolysis, with formation of successive linking disiloxane bonds, according to the reactions:

$$\mathrm{Si{-}OH + OH{-}Si \rightarrow Si{-}O{-}Si + H_2O}$$

$$\mathrm{Si{-}OR + OH{-}Si \rightarrow Si{-}O{-}Si + ROH}$$

According to Iler,[2] the global polymerization process can be divided into three stages: (1) aggregation of small clusters to form sol particles; (2) growth of sol particles; (3) linking of particles into chains, then networks that eventually extend throughout the liquid medium, forming the gel.

Unlike carbon-based polymers, where chains grow and cross-link by covalent branches or van der Waals interactions, highly condensed clusters are formed in silicon-based polymers and particles with 1−500 nm size may be produced. Silicic acid has a strong tendency to form polymers with a maximum of siloxane bonds and a minimum of Si−OH groups.[2] Thus, highly condensed clusters, including ring structures, are formed during the earliest stage of polymerization. These clusters continue to grow by further addition of monomers and by linking together, to form larger three-dimensional structures, which condense internally to the most compact state with Si−OH groups remaining on the outside.

Inductive effects play an important role in the chemistry of silica in solution. The electron-withdrawing effect of the most usual substituents attached to silicon increases in the order R, OR, OH, and OSi, where R represents an alkyl group. Consequently, in both hydrolysis and condensation reactions, electron-providing groups are replaced by electron-withdrawing groups, increasing the acidity of the silanol groups.

The most stable protonated clusters should be the smallest ones, owing to the smaller withdrawing effect of the OH groups. Thus condensation should occur preferentially between neutral, larger clusters and protonated monomers or end groups on chains. Because deprotonated species of the type Si−O−Si−O^- should be more stable than protonated structures, such as $HOSi{-}OH_2^+$, condensation occurs more quickly in basic than in acid conditions. As discussed in the previous article,[1] water- and alcohol-consuming depolymerizations are also much more important under basic conditions than under acid conditions.

The particles formed by such condensation reactions act as nuclei for further polymerization, which occurs by essentially three processes: (1) growth of particles at the expense of silicic acid in solution; (2) an Ostwald Ripening Mechanism, in which small particles, which are more soluble, dissolve and reprecipitate on larger, less soluble, nuclei, so the particles in solution grow in size and decrease in number. Differences in solubility between particles decrease with size, as curvature effects become less significant.[2,3] (3) At low pH, the silica particles are essentially neutral and thus can collide and aggregate forming chains and eventually a gel network.

This article concentrates on the properties of intermediate and larger silica clusters (following our study of smaller species in part I), whose formation will play a crucial role in both sol−gel and hydrothermal syntheses.

† Royal Institution of Great Britain.
‡ University College London.

10.1021/jp982867d CCC: $18.00
Published on Web 04/09/1999

1.1. Experimental Studies. Among the most important work published to date on silica-based clusters in general are the studies of Kelts and Amstrong,[4] using ^{29}Si NMR spectroscopy, and of Klemperer et al.,[5−9] using a combined protocol to separate and measure the clusters: quenching by diazomethane; fractionation using spinning band column distillation; identification by capillary gas chromatography and structural characterization using ^{29}Si NMR.

Klemperer identified the monomer, the dimer, the acyclic trimer, both acyclic tetramers, the cyclic tetramer, the branched cyclic tetramer, the linear and the branched acyclic pentamers and the cyclic pentamer; but the cyclic trimer, the branched cyclic trimer, and the acyclic pentamer cross were not observed. The acyclic linear clusters are clearly more probable than the branched ones. For the 4-Si, 5-Si, and 6-Si clusters, the ratio between linear and branched isomers was found experimentally to be 0.2, 0.6, and 0.008, in acidic conditions (0.05 M HCl[7]). Under basic conditions the cluster distribution is much broader than under acidic conditions.

Knight[10] discussed the structures of the 16 so-called secondary building units (SBUs), the common structural subunits used until 1990 to classify the 64 topologically distinct zeolite networks (the primary building units being single $Si-O_4$ tetrahedra). Comparison of these with the 18 silicate anions determined by ^{29}Si NMR in organic base silicate anions was used to question the utility of the SBU theory.

A complete but older review of the structure of carbon-based rings, with a maximum of 10 carbons, including bridging oxygens and odd-membered rings, was presented by Dunitz and Ibers.[11] The chair, crown, and S-shaped conformations are recognized as the most stable for 6, 8, and 10 carbon rings. No equivalent work is known for silica- or silicon-based cyclic structures. However, the structure and energetics of planar rings in vitreous silica are reviewed by Galeener.[12]

1.2. Previous Theoretical Studies. Several studies have been reported previously in larger silica clusters. Among them are the Hartree−Fock calculations of Hill and Sauer[13] and Moravetski et al.,[14] which include the pentamer and hexamer rings and large cages (prismatic hexamer, cubic octamer, hexagonal dodecamer, sodalite). Hill and Sauer[13] used the data thus acquired to develop a molecular mechanics force field suitable to simulate larger zeolite structures. Self-consistent field (SCF) reaction energies, per mole of Si−O bonds, were presented for the formation of 3-, 4-, 5- and 6-Si rings, respectively, −1.1 kcal mol^{-1}, −3.6 kcal mol^{-1}, −4.1 kcal mol^{-1}, and −4.1 kcal mol^{-1}. Moravetski et al.[14] studied the effect of symmetry and degree of condensation in these clusters and calculated the ^{29}Si magnetic shielding constants to compare with NMR experiments. Hydration effects were also analyzed.

Semiempirical calculations were reported by West et al.[15,16] for rings and chains containing 2, 3, 4, 5, and 6 silica tetrahedra. The adsorption of a water molecule by a four-silicon ring was also analyzed. Lasaga and Gibbs[17,18] also reported ab initio calculations on silicate clusters to obtain potential surfaces for the Si−O bond in silicates. These potential surfaces form the basis for extracting the key parameters in various commonly used potential functions. The geometry of the 5-Si cross, with hydroxyl groups replaced by hydrogens, was optimized by Pápai et al.,[19] at the local density functional (DF) level of theory, using the Vosko−Wilk−Nusair parameterization and the Perdew and Wang nonlocal corrections to evaluate the energies. Finally, molecular dynamics simulations of the silica condensation reactions, forming large silica clusters, were reported by Garofalini and Martin[20] and Feuston and Garofalini.[21,22]

In this article we complete our DF results for all $Si_xO_y(OH)_z$ clusters with a maximum of five silicon atoms and two intramolecular condensations, plus the six-silicon ring and the cube containing eight silicons. DFT is particularly suitable for the study of such large clusters because the computer requirements scale approximately as N^3 compared with approximately N^4 for Hartree−Fock methods. We present the structure, the total condensation energy (from the monomer), and the charge distribution for the more complex clusters. These studies provide the basis for a much better understanding of the chemistry of silica. When comparing the theoretical and experimental results, two important factors should be considered: the terminal oxygen groups and the solvation environment. Although OH groups are easier to handle in theoretical studies, OCH_3 groups are generally present in experimental sol−gel studies because of the small amounts of water used (water and the most commonly used silica alkoxides are immiscible[3]). Although experimental results are obtained under liquid-state conditions, the theoretical results presented here were calculated in gas-phase conditions. A summary of some of the calculations presented here has been presented in a recent review.[23] Ab initio calculations to investigate the influence of the alkoxide groups and the solvation environment in the hydrolysis and condensation reactions will be reported in subsequent publications.

2. Computational Details

All calculations reported in this article were performed with Dmol 2.1−96.0, an ab initio DF code from Molecular Simulations Inc.[24] using a double numerical basis set with polarization functions, and the local density approximation (LDA) at the DF-BHL/DNP level of approximation, as discussed in the previous paper.[1]

The local exchange and correlation energies are calculated separately, using the functional developed by von Barth and Hedin,[25] after Hedin and Lundqvist,[26] and reviewed by Moruzzi et al.[27] Details of Dmol implementation can be found in our previous paper[1] and in refs 24 and 28. All Dmol calculations reported in this paper were carried out using a SCF tolerance of 10^{-5} au for the electronic density, a gradient tolerance of 0.015 au for each coordinate, and a medium grid, as in the previous paper. Full geometry optimization was carried out in all cases. No Basis Set Superposition Errors (BSSE) or zero-point energy corrections were introduced.

3. Results

The most relevant energetic and structural information obtained from our calculations is now considered in detail. First, we analyze the branched four- and five-silicon clusters and compare them with the linear clusters (discussed in the previous paper[1]) to discuss the effects of branching.

Next we analyze the branched rings, first the trimer and tetramer rings with a lateral chain containing one silicon atom and then the four trimer rings containing two silicons in lateral chains, including (1) a single lateral chain with two silicons; (2) two lateral chains with one silicon each, attached to the same silicon in the ring; (3) two lateral chains with one silicon each, attached to different silicons in the ring, either in the same or in opposite sides of the ring.

We then discuss the double rings, containing a trimer−trimer or tetramer−trimer structure. We start with the trimer−trimer clusters, simple or with a lateral chain containing one silicon, attached either in a central or in a outer position. The special

TABLE 1: Bond Lengths (Å) for Optimized Silica Clusters (O_b = Bridging Oxygen; O_t = Terminal Oxygen; O−H = Hydrogen Bond)

		Si−O_b	Si−O_t	OH	O−H
•	Q_1^0		1.64	0.99	
—	Q_2^1	1.65	1.63−1.66	0.98−1.00	1.91
∧	$Q_2^1\,Q_1^2$	1.63	1.62−1.68	0.98−1.02	1.63−1.65
△	Q_3^2	1.65−1.66	1.62−1.66	0.98−1.00	1.93−1.99
⩘	$Q_2^2\,Q_2^1$	1.64−1.66	1.62−1.67	0.98−1.03	1.51−1.68
⅄	$Q_3^1\,Q_1^3$	1.63−1.66	1.62−1.67	0.98−1.02	1.63−2.02
⅄	$Q_2^2\,Q_1^3\,Q_1^1$	1.61−1.67	1.62−1.66	0.98−1.01	1.85−2.20
◇	$Q_2^3\,Q_2^2$	1.63−1.66	1.62−1.65	0.98−1.00	2.04
□	Q_4^2	1.64−1.65	1.62−1.66	0.98−1.03	1.61−1.62
⩘⩘	$Q_3^2\,Q_2^1$	1.62−1.66	1.61−1.67	0.98−1.02	1.60−1.68
⅄⩘	$Q_3^1\,Q_1^3\,Q_1^2$	1.62−1.65	1.61−1.67	0.98−1.02	1.57−1.73
+	$Q_4^1\,Q_1^4$	1.63−1.68	1.62−1.66	0.98−1.01	1.76−2.04
▷⌐	$Q_2^2\,Q_1^3\,Q_1^2\,Q_1^1$	1.63−1.66	1.63−1.65	0.98−1.00	1.94−2.02
⋊	$Q_2^2\,Q_2^1\,Q_1^4$	1.61−1.66	1.62−1.66	0.98−1.01	1.66
▷—	$Q_2^3\,Q_2^1\,Q_1^2c$	1.62−1.66	1.63−1.67	0.98−1.00	1.86−1.90
▷⋯	$Q_2^3\,Q_2^1\,Q_1^2t$	1.61−1.66	1.63−1.65	0.98−1.00	1.78−1.97
◇	$Q_2^3\,Q_1^3\,Q_1^2\,Q_1^1$	1.63−1.66	1.62−1.66	0.98−1.01	1.75−1.94
◇—	$Q_2^2\,Q_1^4\,Q_1^3\,Q_1^1$	1.61−1.66	1.62−1.66	0.98−1.01	1.72
⋈	$Q_4^2\,Q_1^4$	1.62−1.67	1.62−1.66	0.98−1.01	1.72−1.88
□⌐	$Q_3^2Q_1^3Q_1^1$	1.61−1.66	1.62−1.66	0.98−1.03	1.62−1.65
□▷	$Q_2^2Q_2^3Q_1^2e$	1.63−1.65	1.62−1.67	0.98−1.02	1.63−1.64
◪	$Q_2^2\,Q_2^3\,Q_1^2c$	1.62−1.66	1.63−1.65	0.98−1.00	1.81−1.82
⬠	Q_5^2	1.62−1.66	1.62−1.66	0.98−1.02	1.64−1.84
⬡	Q_6^2	1.64−1.65	1.63−1.66	0.98−1.04	1.56−1.60
⧈	Q_8^3	1.63−1.64	1.63	0.98	

trimer−trimer cluster where both rings are linked by a single silicon atom is presented next, together with the two tetramer−trimer clusters, bonded either by an edge or by corners.

Finally, we analyze the larger clusters, the five- and six-silicon rings. We present first the lowest energy conformation and discuss the energetics for each cluster, before analyzing together the structural details of each class of clusters.

All silica clusters discussed here are shown in Figures 1 through 7, including the most relevant energy, structure, and charge distribution information. As in part I, for each cluster there are three tables: one for bond lengths, another for bond angles, and another for charges. The abbreviated notation used in part I is used in all tables. We recall that O_b and O_t denote bridging and terminal oxygen, respectively.

Silica clusters are classified in this work according to the NMR notation, Q_n^m, where n represents the number of silicons that are bonded to m bridging oxygens. Different groups are ordered according to the parameter n first and m second; when groups with equal m have different chemical environments they are explicitly separated (as in $Q_2^2\,Q_1^3\,Q_1^2\,Q_1^1$). When this notation was insufficient we used *e*, *c*, *t* for edge, corner, cis and trans specifications. Total and reactional energies, bond lengths and bond angles, charge distribution and electric dipoles, for all silica clusters, are summarized in Tables 1−4. Bond lengths and bond angles are presented in Tables 1 and 2, whereas the charge distribution and the electric dipole moments are shown in Table 3. The total energy and the condensation energy to form each cluster from the monomer are given in Table 4. Calculated and corrected values (subtracting 3.3 kcal mol^{-1} per H-bond when O− H < 1.85 Å, as discussed in ref 1), divided by the number n of condensation reactions to form the cluster and the number s of silicon atoms in the cluster are also given.

TABLE 2: Bond Angles (degrees) for Optimized Silica Clusters (O_b = Bridging Oxygen; O_t = Terminal Oxygen)

		Si−O−Si	O_b−Si−O_b	O_t−Si−O_t	Si−OH
	Q_1^0			105.6−117.6	112.4
	Q_2^1	118.4		110.7−114.0	107.7−113.5
	$Q_2^1\,Q_1^2$	138.4−144.2	113.2	106.7−112.6	111.1−115.7
	Q_3^2	115.7−116.1	107.9−108.8	112.9−114.4	106.6−114.8
	$Q_2^2\,Q_2^1$	121.7−128.0	108.5−109.7	106.8−112.5	104.7−118.0
	$Q_3^1\,Q_1^3$	117.3−123.7	109.2−110.7	104.4−113.7	107.9−114.8
	$Q_2^2\,Q_1^3\,Q_1^1$	115.2−123.2	106.7−111.0	113.5−115.2	106.5−114.7
	$Q_2^3\,Q_2^2$	112.8−127.2	107.2−110.1	106.0−109.0	112.5−115.0
	Q_4^2	125.8−126.3	111.2−112.2	113.2−114.8	106.2−114.3
	$Q_3^2\,Q_2^1$	130.4−159.2	105.8−116.1	106.6−112.4	110.0−117.7
	$Q_3^1\,Q_1^3\,Q_1^2$	124.0−147.0	105.7−109.7	106.6−111.8	108.9−124.8
	$Q_4^1\,Q_1^4$	119.8−122.8	110.5−113.9	107.2−111.2	110.9−113.2
	$Q_2^2\,Q_1^3\,Q_1^2\,Q_1^1$	117.5−123.7	106.9−111.5	109.7−114.4	107.3−114.0
	$Q_2^2\,Q_2^1\,Q_1^4$	122.8−133.0	107.9−110.6	106.3−116.7	111.4−118.1
	$Q_2^3\,Q_2^1\,Q_1^2c$	116.0−124.2	105.5−114.1	108.4−110.3	107.8−113.7
	$Q_2^3\,Q_2^1\,Q_1^2t$	115.5−130.1	105.3−111.5	106.7−116.6	110.2−113.9
	$Q_2^3\,Q_1^3\,Q_1^2\,Q_1^1$	113.3−127.5	105.9−111.7	108.5−110.1	109.1−114.5
	$Q_2^2\,Q_1^4\,Q_1^3\,Q_1^1$	113.3−129.2	106.6−112.1	106.0−110.0	111.1−114.6
	$Q_4^2\,Q_1^4$	114.7−122.8	105.4−109.2	111.0−115.3	105.2−115.6
	$Q_3^2\,Q_1^3\,Q_1^1$	124.7−126.6	109.1−112.5	108.6−115.9	106.2−115.1
	$Q_2^2\,Q_2^3\,Q_1^2e$	125.9−148.2	106.0−130.4	104.5−112.8	111.5−115.1
	$Q_2^2\,Q_2^3\,Q_1^2c$	126.6−140.9	106.6−117.6	108.0−114.3	111.5−120.1
	Q_5^2	116.3−136.1	107.2−111.0	103.9−115.9	106.7−115.0
	Q_6^2	127.1−130.0	110.5−112.3	113.0−114.9	106.4−115.3
	Q_8^3	136.3−138.0	110.1−111.2		113.8−113.9

3.1. Branching Effects: Branched Four- and Five-Silicon Clusters. In this section we study the branched noncyclic clusters, which contain four and five silicon atoms. Our results show that the branched clusters have higher energy than the linear clusters, and should therefore be less stable, in agreement with experiment.

3.1.1. Branched Four-Silicon Cluster. The structure and charge distribution of the noncyclic four-silicon clusters are presented in Figure 1. The proposed conformation for the branched tetramer (above, in the figure) has four hydrogen bonds: two have a reasonable O- -H distance (1.80 and 2.02 Å) but the other two are too short (1.63−1.64 Å). The corresponding OH bond lengths seem also to be acceptable for the former two H-bonds (1.00 Å) but slightly large in the latter two (1.01−1.02 Å). Although the condensation energy for the branched tetramer is considerably negative (−30.6 kcal mol^{-1}), it is less negative by 7.5 kcal mol^{-1} than for the linear cluster (discussed in the previous paper). This result is in agreement with the experimental evidence, which shows that it is much easier to form the linear than the branched tetramer.[7] However, because there are five apparently overestimated H-bonds in the linear tetramer against only two in the branched tetramer, after applying the correction of 3.3 kcal mol^{-1} per H-bond, the energy becomes lower for the branched cluster (−24.0 kcal mol^{-1}) than for the linear cluster (−21.7 kcal mol^{-1}). Although the corrected energies seem to be more reasonable, the effect of the correction is such that we cannot draw any reliable conclusion about the relative stability of the two clusters. At the LDA level of approximation, the charge separation is very similar in the linear (2.75 D) and in the branched (2.60 D) clusters.

3.1.2. Branched Five-Silicon Cluster. The structure and charge distribution of the noncyclic five-silicon clusters are presented in Figure 2. The most stable conformation found for the branched five-silicon cluster (in the middle, Figure 2) has

TABLE 3: Dipole (Dip.) Moment (Debye) and Hirshfeld Atomic Charges for Optimized Silica Clusters (O_b = Bridging Oxygen; O_t = Terminal Oxygen)

		Dip.	Si	O_b	O_t	H
•	Q_1^0	0.00	0.8660		−0.7620	0.5460
—	Q_2^1	1.09	0.4598	−0.2777	−0.2433, −0.2935	0.1212, 0.1839
∧	$Q_2^1 Q_1^2$	0.35	0.4648, 0.4733	−0.2685	−0.2195, −0.3005	0.0954, 0.1878
△	Q_3^2	1.68	0.4731, 0.4764	−0.2703, −0.2734	−0.2557, −0.2643	0.1253, 0.1877
∧	$Q_2^2 Q_2^1$	2.75	0.4611, 0.4852	−0.2151, −0.2737	−0.2313, −0.2907	0.1038, 0.1823
⅄	$Q_3^1 Q_1^3$	2.60	0.4620, 0.4750	−0.2437, −0.2686	−0.2171, −0.3003	0.0948, 0.1929
△	$Q_2^2 Q_1^3 Q_1^1$	1.93	0.4617, 0.4861	−0.2465, −0.2701	−0.2376, −0.2913	0.1224, 0.1900
◇	$Q_2^3 Q_2^2$	2.82	0.4695, 0.4773	−0.2640, −0.2817	−0.2438, −0.2831	0.1304, 0.1869
□	Q_4^2	0.65	0.4818, 0.4851	−0.2655, −0.2699	−0.2440, −0.2648	0.1070, 0.1861
∧∧	$Q_3^2 Q_2^1$	3.23	0.4579−0.4890	−0.2559, −0.2734	−0.2120, −0.2930	0.0958, 0.1916
⅄	$Q_3^1 Q_1^3 Q_1^2$	3.75	0.4541, 0.4956	−0.2583, −0.2795	−0.2184, −0.3043	0.0918, 0.1972
+	$Q_4^1 Q_1^4$	0.23	0.4571, 0.4856	−0.2609, −0.2628	−0.2212, −0.2905	0.1042, 0.1957
▷	$Q_2^2 Q_1^3 Q_1^2 Q_1^1$	1.78	0.4607, 0.4767	−0.2579, −0.2757	−0.2432, −0.2891	0.1253, 0.1885
⋈	$Q_2^2 Q_2^1 Q_1^4$	2.06	0.4588, 0.4920	−0.2517, −0.2698	−0.2115, −0.2966	0.0982, 0.1908
▷	$Q_2^3 Q_2^1 Q_1^2 c$	1.28	0.4573, 0.4781	−0.2493, −0.2678	−0.2337, −0.2914	0.1229, 0.1871
▷	$Q_2^3 Q_2^1 Q_1^2 t$	2.52	0.4611, 0.4861	−0.2601, −0.2695	−0.2246, −0.2964	0.1129, 0.1956
◇	$Q_2^3 Q_1^3 Q_1^2 Q_1^1$	2.51	0.4643, 0.4825	−0.2579, −0.2790	−0.2275, −0.2934	0.1052, 0.1878
◇	$Q_2^2 Q_1^4 Q_1^3 Q_1^1$	3.36	0.4647, 0.4893	−0.2516, −0.2713	−0.2164, −0.2954	0.1017, 0.1956
⋈	$Q_4^2 Q_1^4$	3.84	0.4691, 0.4860	−0.2502, −0.2732	−0.2402, −0.2856	0.0997, 0.1919
□	$Q_3^2 Q_1^3 Q_1^1$	1.88	0.4601, 0.4892	−0.2417, −0.2664	−0.2353, −0.2898	0.1078, 0.1869
□	$Q_2^2 Q_2^3 Q_1^2 e$	2.54	0.4615, 0.4869	−0.2644, −0.2737	−0.2451, −0.2990	0.0945, 0.1955
□	$Q_2^2 Q_2^3 Q_1^2 c$	5.99	0.4617, 0.4838	−0.2567, −0.2743	−0.2312, −0.2888	0.1037, 0.1926
⬠	Q_5^2	3.39	0.4629, 0.4893	−0.2504, −0.2786	−0.2061, −0.2824	0.1033, 0.1878
⬡	Q_6^2	0.82	0.4816, 0.4886	−0.2615, −0.2650	−0.2380, −0.2712	0.1064, 0.1841
⧈	Q_8^3	0.06	0.4842, 0.4847	−0.2601, −0.2705	−0.2699, −0.2707	0.1814, 0.1819

four hydrogen bonds, probably overestimated (O- -H = 1.64−1.72 Å), forming three secondary rings with 8 atoms each. The condensation energy (−40.2 kcal mol^{-1}) is 3.4 kcal mol^{-1} less favorable than for the linear chain, decreasing to −27.0 kcal mol^{-1}, when corrected for the hydrogen bonds (compared with −30.4 kcal mol^{-1} for the linear chain). The corrected energy is probably a reasonable estimate, when compared with the values obtained for the previous clusters, particularly the noncyclic ones.

The dipole moment of the branched pentamer is even larger (3.75 D) than in the five-silicon linear chain (discussed in the previous paper). However, the calculated dipole moments (particularly for larger, less constrained, and therefore more complex clusters) are probably not very reliable at this level of approximation (LDA with a double basis set), as suggested by the monomer and dimer studies discussed in part I.[1]

3.1.3. Pentamer Cross. In the pentamer cross (see Figure 2, above), a central silicon is attached to four bridging oxygens, each one subsequently bonded to a terminal $Si(OH)_3$, forming a highly symmetric structure, which has an almost zero dipole moment, 0.23 D. The lowest energy conformation found for this cluster has four hydrogen bonds formed by terminal hydroxyl groups, forming four secondary rings, plus two other hydrogen bonds formed by bridging oxygens, forming four additional secondary rings. The cluster is therefore a good precursor to produce the double branched three-silicon ring, by forming an intramolecular Si−O−Si disiloxane bond. Three of the hydrogen bonds have O−H distances that are too short (1.76−1.83 Å), whereas the others are normal (O- -H = 2.04−2.14 Å) or even weak (2.57 Å).

The condensation energy for the pentamer cross, although relatively large (−32.0 kcal mol^{-1}), is still 8.2 kcal mol^{-1}

TABLE 4: Total Energy (TE) for Each Optimized Silica Cluster (in Hartree), plus Calculated (CA) and Corrected (CO) Total Condensation Energy to Form the Cluster from the Monomer (in kcal mol^{-1}), Divided by the Number of Condensation Reactions Required to Form the Cluster (n) or by the Number of Silicons in the Cluster (s)[a]

		TE	CA(CO)	CA(CO)/*n*	CA(CO)/*s*	
•	Q_1^0	−589.89392				1 Si
—	Q_2^1	−1103.8924	−9.4 (−2.8)	−9.4 (−2.8)	−4.7 (−1.4)	2 Si
∧	$Q_2^1 Q_1^2$	−1617.8905	−18.5 (−11.9)	−9.3 (−6.0)	−6.2 (−4.0)	3 Si
△	Q_3^2	−1541.9532	−1.6 (−1.6)	−0.5 (−0.5)	−0.5 (−0.5)	
∧∨	$Q_2^2 Q_2^1$	−2131.9053	−38.2 (−21.7)	−12.7 (−7.2)	−9.5 (−5.4)	4 Si
⅄	$Q_3^1 Q_1^3$	−2131.8933	−30.6 (−24.0)	−10.2 (−8.0)	−7.7 (−6.0)	
△	$Q_2^2 Q_1^3 Q_1^1$	−2055.9436	−6.0 (−6.0)	−1.5 (−1.5)	−1.5 (−1.5)	
◇	$Q_2^3 Q_2^2$	−1980.0136	+6.4 (+6.4)	+1.3 (+1.3)	+1.6 (+1.6)	
□	Q_4^2	−2055.9751	−25.7 (−12.5)	−6.4 (−3.1)	−6.4 (−3.1)	
∧∧	$Q_3^2 Q_2^1$	−2645.8975	−43.6 (−30.4)	−10.9 (−7.6)	−8.7 (−6.1)	5 Si
⅄∨	$Q_3^1 Q_1^3 Q_1^2$	−2645.8921	−40.2 (−27.0)	−10.1 (−6.8)	−8.0 (−5.4)	
+	$Q_4^1 Q_1^4$	−2645.8790	−32.0 (−22.1)	−8.0 (−5.5)	−6.4 (−4.4)	
▷∕	$Q_2^2 Q_1^3 Q_1^2 Q_1^1$	−2569.9351	−11.0 (−11.0)	−2.2 (−2.2)	−2.2 (−2.2)	
▷◁	$Q_2^2 Q_2^1 Q_1^4$	−2569.9356	−11.3 (−11.3)	−2.3 (−2.3)	−2.3 (−2.3)	
▷	$Q_2^3 Q_2^1 Q_1^2 c$	−2569.9351	−11.0 (−11.0)	−2.2 (−2.2)	−2.2 (−2.2)	
▷	$Q_2^3 Q_2^1 Q_1^2 t$	−2569.9343	−10.5 (−7.2)	−2.1 (−1.4)	−2.1 (−1.4)	
◇	$Q_2^3 Q_1^3 Q_1^2 Q_1^1$	−2494.0106	−2.1 (+1.2)	−0.4 (−0.2)	−0.4 (−0.2)	
◇—	$Q_2^2 Q_1^4 Q_1^3 Q_1^1$	−2494.0076	−0.2 (+3.1)	−0.0 (+0.5)	−0.0 (+0.6)	
⋈	$Q_4^2 Q_1^4$	−2494.0098	−1.6 (+1.7)	−0.3 (+0.3)	−0.3 (+0.3)	
□∕	$Q_3^2 Q_1^3 Q_1^1$	−2569.9670	−31.0 (−17.8)	−6.2 (−3.6)	−6.2 (−3.6)	
□▷	$Q_2^2 Q_2^3 Q_1^2 e$	−2494.0289	−13.6 (−7.0)	−2.3 (−1.2)	−2.7 (−1.4)	
□◹	$Q_2^2 Q_2^3 Q_1^2 c$	−2494.0209	−8.6 (−2.0)	−1.4 (−0.3)	−1.7 (−0.4)	
⬠	Q_5^2	−2569.9577	−25.2 (−18.5)	−5.0 (−3.7)	−5.0 (−3.7)	
⬡	Q_6^2	−3083.9788	−48.7 (−28.9)	−8.1 (−4.8)	−8.1 (−4.8)	6 Si
⧈	Q_8^3	−3808.2202	+4.1 (+4.1)	+0.3 (+0.3)	+0.5 (+0.5)	8 Si

[a] Corrected energies (after subtracting 3.3 kcal/mol^{-1} per H-bond with O--H < 1.85 Å) are discussed in part I.[1]

smaller than for the branched chain (−40.2 kcal mol^{-1}). Taking into account the three overestimated hydrogen bonds, the corrected energy is estimated as −22.1 kcal mol^{-1}, smaller than the corrected energy (−27.0 kcal mol^{-1}) for the branched pentamer. Because the condensation energy for the branched pentamer is, in turn, smaller than for the linear chain, it can be concluded that, the cluster stability decreases with the degree of branching, at the LDA level of approximation, in agreement with the experimental evidence.

The pentamer cross is the only cluster studied in this work where a silicon atom is bonded to four unconstrained bridging oxygens. It is therefore relevant to compare the SiO_4 central atoms with those in terminal $Si(OH)_3$ groups and in $Si(OH)_4$. The Hirshfeld charges are very similar in both cases. The Mulliken charge in the central silicon is larger (+1.152) than in the terminal Si atoms (0.988 to 1.064); the bridging oxygens have much smaller charges (−0.557 to −0.625) than in the terminal OH groups (−0.723 to −0.845).

3.1.4. Structures. As observed for other clusters (see previous paper[1]), the Si−O and O−H bond lengths vary considerably with the bonding characteristics of the hydroxyl groups, changing from 1.61−1.63 Å and 1.00−1.02 Å in acceptor groups (where the hydrogen forms a hydrogen bond, therefore receiving charge) to 1.65−1.67 and 0.99 Å in donor groups (where the oxygen forms an hydrogen bond, therefore donating charge). Hydroxyl groups participating simultaneously in two different hydrogen bonds (where the hydrogen accepts charge, whereas the oxygen donates it) tend to have intermediate bond

Si 4620-4750	*SiO$_b$* 1.63-1.66	*SiOSi* 117.3-123.7
O$_b$ 2437-2686	*SiO$_t$* 1.62-1.67	*O$_b$SiO$_b$* 109.2-110.7
O$_t$ 2171-3003	*OH* 0.98-1.02	*O$_t$SiO$_t$* 104.4-113.7
H 0948-1929	*O-H* 1.63-2.02	*SiOH* 107.9-114.8

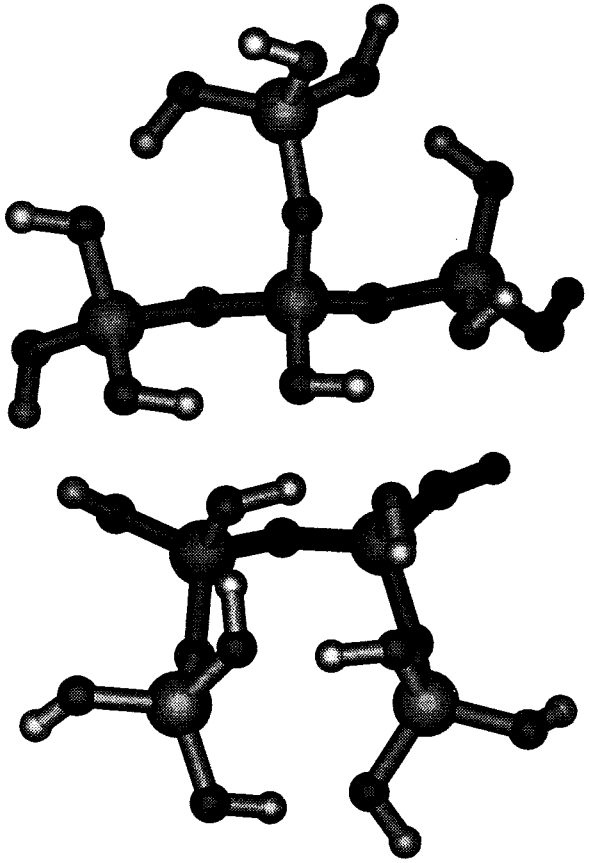

Si 4611-4852	*SiO$_b$* 1.64-1.66	*SiOSi* 121.7-128.0
O$_b$ 2151-2737	*SiO$_t$* 1.62-1.67	*O$_b$SiO$_b$* 108.5-109.7
O$_t$ 2313-2907	*OH* 0.98-1.03	*O$_t$SiO$_t$* 106.8-112.5
H 1038-1823	*O-H* 1.51-1.68	*SiOH* 104.7-118.0

Figure 1. Bond lengths (Å), bond angles (degrees), and Hirshfeld atomic charges (0. and minus signal in O charges are omitted) for noncyclic four-silicon clusters, optimized at the DF-BHL/DNP level of approximation. Total energy: E = −2131.9053 Ha ($Q_2^2\,Q_1^2$) and $E = -2131.8933$ Ha ($Q_3^1\,Q_1^3$). Dipole moment: $\mu = 2.75$ D ($Q_2^2\,Q_1^2$) and $\mu = 2.60$ D ($Q_3^1\,Q_1^3$).

lengths (1.66 and 1.01 Å), which are slightly longer than in the terminal, unconstrained OH groups (1.63−1.64 Å and 0.98−0.99 Å).

In the open, highly symmetric, pentamer cross, the central Si−O$_b$ bonds are slightly shorter (1.63−1.64 Å) than the terminal Si−O$_b$ bonds (1.64−1.68 Å), which agrees with the experimental and theoretical evidence that the Si−O bond length tends to decrease in more bridged systems. The Si−O bond length in α quartz, for instance (1.60 Å[29]), is smaller than the reference value for Si(OH)$_4$ in the gas-phase (of about 1.62 Å[30]).

For all three clusters, the relatively hard O$_b$−Si−O$_b$ angles are almost constant (around 113.7°), but the Si−O−Si and O$_t$−Si−O$_t$ angles change considerably: 117.3−138.3° and 104.4−113.7°) in the branched tetramer. The Si−O−Si angles might be about 10−15 degrees too small, taking into account the results with different basis sets obtained for the dimer and experimental evidence on vitreous silica.[31]

3.2. Branched Rings: One-Silicon Branched Trimer and Tetramer Rings. In this section we analyze the simplest branched rings, the trimer and tetramer rings containing a one-silicon lateral chain. Both clusters have a relatively negative condensation reaction energy (from the monomer) and keep the "chair" and "crown" conformations previously found for the non-branched rings.

3.2.1. Branched Trimer Ring. The structure and charge distribution of the branched trimer and tetramer rings, are shown in Figure 3. The branched trimer ring (above, in the figure) results from the association of a trimer ring (in a chair conformation) with a monomer (in an S_4 conformation), arranged in such a way that a bridging oxygen in the ring forms a H-bond with the Si(OH)$_3$ chain. This H-bond is weaker (1.91 Å) than the three H-bonds in the ring (O- -H = 1.85−2.20 Å), which are distorted slightly by the influence of the lateral chain.

The condensation energy of −6.0 kcal mol^{-1} is 4.4 kcal mol^{-1} lower than for the three-silicon ring, and although it is relatively small because of the ring strain, it is sufficiently negative to justify the significant concentration of this cluster usually found in sol−gel solutions.[4,10] As in other clusters with a trimer ring,

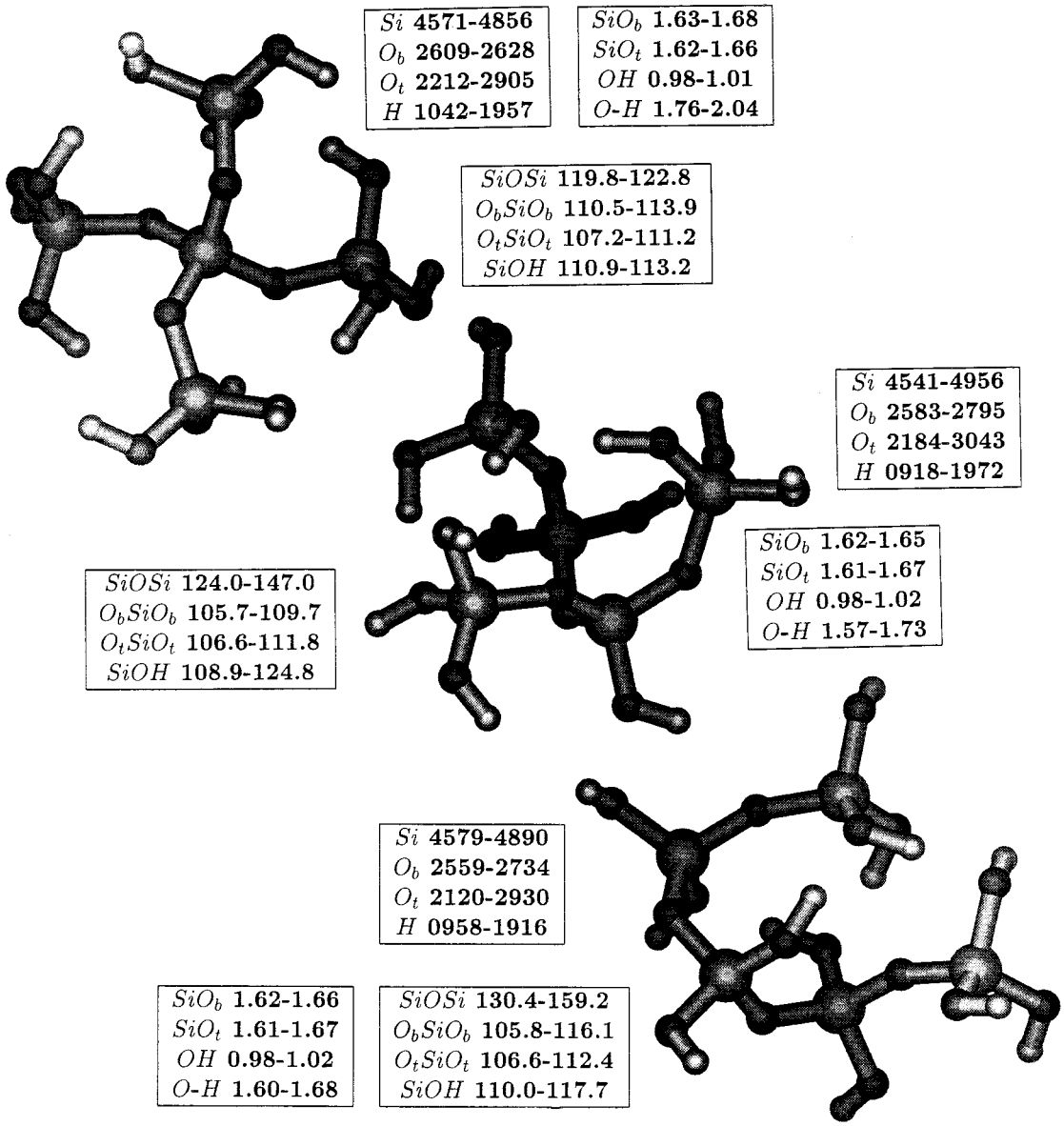

Figure 2. Bond lengths (Å), bond angles (degrees), and Hirshfeld atomic charges (0. and minus signal in O charges are omitted) for noncyclic five-silicon clusters, optimized at the DF-BHL/DNP level of approximation. Total energy: $E = -2645.8975$ Ha ($Q_3^2\,Q_1^2$), $E = -2645.8921$ Ha ($Q_3^1\,Q_1^3\,Q_1^2$) and $E = -2645.8790$ Ha ($Q_4^1\,Q_1^4$). Dipole moment: $\mu = 3.23$ D ($Q_3^2\,Q_1^2$), $\mu = 3.75$ D ($Q_3^1\,Q_1^3\,Q_1^2$) and $\mu = 0.23$ D ($Q_4^1\,Q_1^4$).

the electric dipole is relatively high (1.93 Å), an effect probably enhanced by the separation between the ring and the chain.

3.2.2. Branched Tetramer Ring. The branched tetramer ring (see Figure 3, below) is formed by associating a tetramer ring (in a crown conformation) with an S_4 monomer, thus preserving most of the features of these clusters. The lateral chain adds a further hydrogen bond (O- -H = 1.96 Å) to the four hydrogen bonds in the ring (O- -H = 1.62−1.65 Å), considerably increasing the rigidity of the cluster, because the lateral chain can no longer rotate.

The condensation energy for this cluster of −31.0 kcal mol^{-1} is 5.3 kcal mol^{-1} lower than for the four-silicon ring and is considerably negative, because of the five H− bonds. When corrected for the four overestimated H-bonds, the energy is estimated as −17.8 kcal mol^{-1}, which is probably more reasonable.

The dipole moment for the branched tetramer ring (1.88 D) is much higher than in the four-silicon ring (0.65 D), which seems to confirm that a lateral chain in a ring tends to increase substantially the charge separation.

3.2.3 Structures. In the branched three-silicon ring, the Si−O_b bond lengths in the ring (1.65−1.67 Å) and the Si−O, OH bond lengths in the chain (1.63−1.64 and 0.98 Å) are very close to the corresponding values in the trimer ring and in the monomer. The transition between the ring and the lateral chain is characterized by the additional hydrogen bond, which introduces a second link between the ring and the chain, this way increasing considerably the rigidity of the cluster. The Si−O bond linking the ring and the chain is much shorter (1.61 Å) than the others in the ring (1.64−1.67 Å) or in the chain (1.63−1.67 Å). In the four-silicon ring, the Si−O bond length is much smaller (1.62 Å) than the corresponding values in open chains (1.64 Å).

As in the monomer, the O_t−Si−O_t angle in the branched trimer ring has two different values in the chain (≈109.2° (2×) and 115.2° (perpendicular to the main chain)), whereas it is essentially constant in the ring (113.6−114.3°). The Si−O−Si angle in the branched tetramer ring is almost constant and changes even less than the much harder O_b−Si−O_b angle because of the high symmetry of the ring.

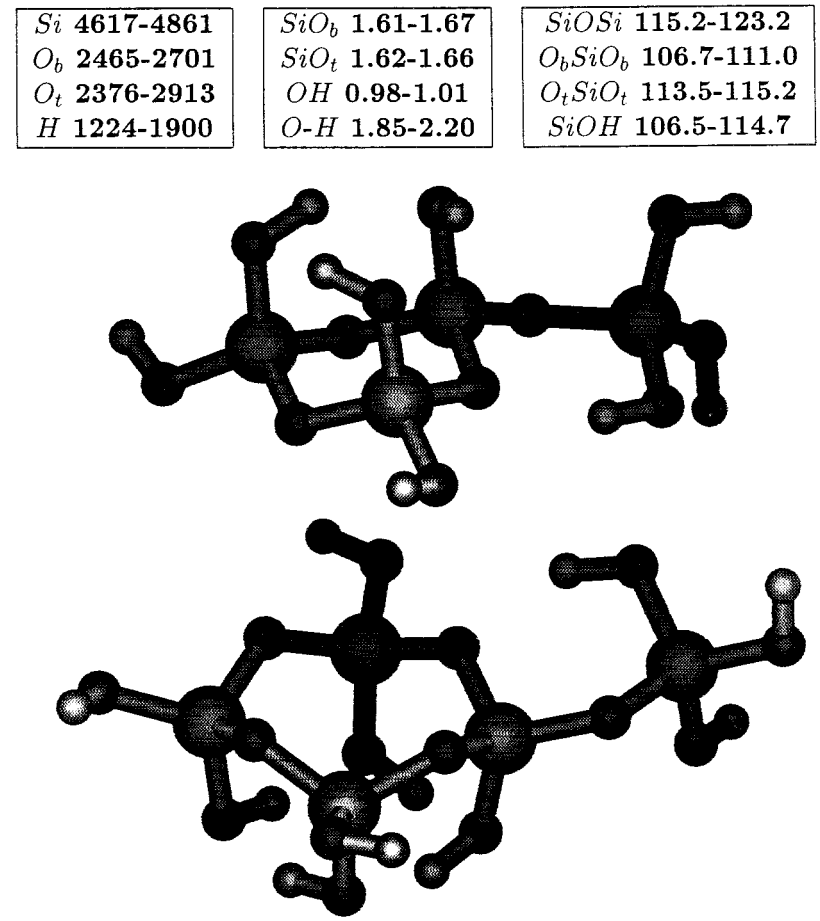

Figure 3. Bond lengths (Å), bond angles (degrees), and Hirshfeld atomic charges (0. and minus signal in O charges are omitted) for $Q_2^2\,Q_1^3\,Q_1^1$ and $Q_3^2\,Q_1^3\,Q_1^1$, optimized at the DF-BHL/DNP level of approximation. Total energy: E = −2055.9436 Ha ($Q_2^2\,Q_1^3\,Q_1^1$) and $E = -2569.9670$ Ha ($Q_3^2\,Q_1^3\,Q_1^1$). Dipole moment: $\mu = 1.93$ D ($Q_2^2\,Q_1^3\,Q_1^1$) and $\mu = 1.88$ D ($Q_3^2\,Q_1^3\,Q_1^1$).

In both clusters, the Si−OH angle is much larger in the free OH groups (≈111−115°) than in the OH groups involved in hydrogen bonds (≈107−111°).

3.3. Branched Rings: Two-Silicon Branched Trimer Rings. We now analyze the four trimer rings containing two silicon atoms in lateral chains. These clusters have similar energies and structural features and should be slightly more stable than the trimer ring.

3.3.1. Single Branched Trimer Ring. The structures and charge distributions of the trimer rings, with two silicon atoms in lateral chains, are presented in Figure 4. The trimer ring with a single two-silicon chain (above right, in the Figure) is formed by associating the ring (in the chair conformation) with a dimer (in the C_2 conformation), arranged to allow the formation of three hydrogen bonds (two in the lateral chain and one between the chain and the ring), increasing considerably the rigidity of the cluster. The corresponding O−H distances are reasonable (1.94−2.02 Å) and consequently the calculated condensation energy (−11.0 kcal mol^{-1}) is probably accurate enough not to need any correction. The dipole moment is relatively small in this cluster (1.78 D, only 0.1 D larger than in the three-silicon ring), which is surprising, because the lateral chain extends the cluster size considerably (to 11.46 Å).

3.3.2. Trans-Branched Trimer Ring. In the *trans*-branched trimer ring (see Figure 4, below right), two lateral chains with one silicon each, are attached to different silicons, on different sides of the ring. There are three hydrogen bonds in this cluster (O−H = 1.85−1.97 and 1.78 Å); the last one is apparently strong. However, the differences between the various hydroxyl groups are smaller than in previous clusters. Furthermore, the Si−O−H angles are almost equal for terminal and H-bond forming OH groups (111.0−113.9° and 110.6−112.4°).

The condensation energy for this cluster (−10.5 kcal mol^{-1}) is only 0.5 kcal mol^{-1} higher than in the previous cluster, but the difference increases after correcting the energy (to −7.2 kcal mol^{-1}), to take into account one possibly overestimated H-bond. The dipole moment is also much larger in this cluster (2.52 D), than in the previous one, apparently because of charge separation effected by the two chains on different sides of the ring.

3.3.3. Cis-Branched Trimer Ring. The *cis*-branched trimer ring (see Figure 4, below left) differs from the previous cluster because the two lateral chains are on the same side of the ring, forming three strong H-bonds (O−H = 1.86−1.90 Å) and a fourth one that is very weak (O−H = 2.74 Å).

The condensation energy for the *cis*-branched cluster (−11.0 kcal mol^{-1}) is almost identical with the energy calculated for

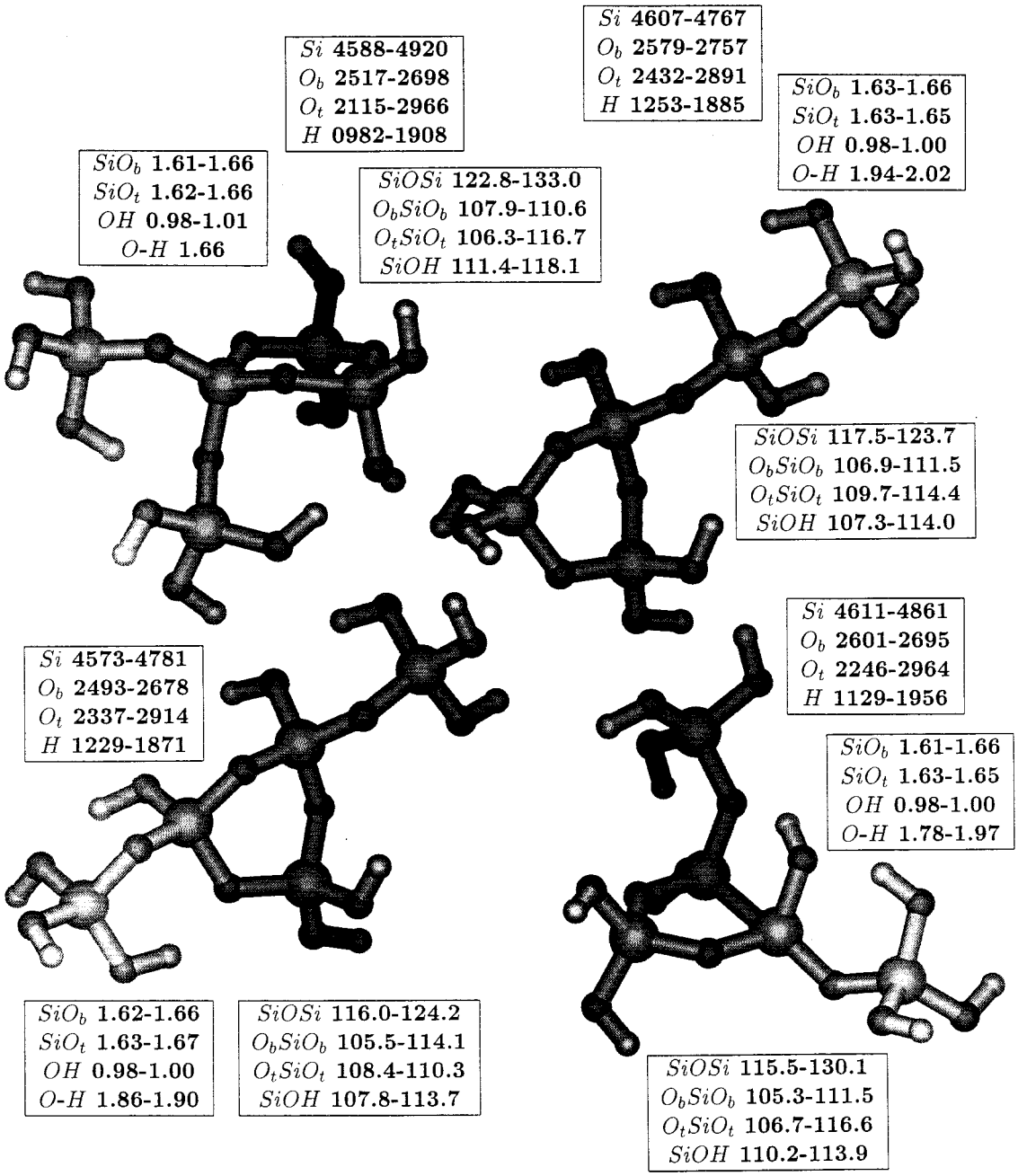

Figure 4. Bond lengths (Å), bond angles (degrees), and Hirshfeld atomic charges (0. and minus signal in O charges are omitted) for $Q_2^2\,Q_1^3\,Q_1^2\,Q_1^1$, $Q_2^2Q_2^1Q_1^4$, $Q_2^3Q_2^1Q_1^2c$ and $Q_2^3Q_2^1Q_1^2t$, optimized at the DF-BHL/DNP level of approximation. Total energy: $E = -2569.9351$ Ha ($Q_2^2\,Q_1^3\,Q_1^2\,Q_1^1$), $E = -2569.9356$ Ha ($Q_2^2\,Q_2^1\,Q_1^4$), $E = -2569.9351$ Ha ($Q_2^3\,Q_2^1\,Q_1^2c$) and $E = -2569.9343$ Ha ($Q_2^3\,Q_2^1\,Q_1^2t$). Dipole moment: $\mu = 1.78$ D ($Q_2^2\,Q_1^3\,Q_1^2\,Q_1^1$), $\mu = 2.06$ D ($Q_2^2\,Q_2^1\,Q_1^4$), $\mu = 1.28$ D ($Q_2^3\,Q_2^1\,Q_1^2c$) and $\mu = 2.52$ D ($Q_2^3\,Q_2^1\,Q_1^2t$).

the *trans*-branched cluster and matches exactly the energy obtained for the trimer ring with a two-silicon chain, suggesting that, regarding energetics, the structural differences between these clusters are not relevant. The *trans*-cluster is 3.8 kcal mol^{-1} less stable after correcting its overestimated H-bonds, but it is not clear whether the correction is accurate in this case.

The electric dipole is relatively small in this cluster (1.28 D), essentially because the relative disposition of the two chains, opposite each other on each side of the ring, increases considerably the symmetry of the whole cluster.

3.3.4. Double-Branched Trimer Ring. In the double-branched trimer ring (see Figure 4, above left), two lateral chains are attached to the same silicon atom in the ring, forming two hydrogen bonds (O- -H = 1.66 and 1.96 Å), the first one probably being overestimated.

The condensation energy (−11.3 kcamol^{-1}) is calculated as or slightly more negative than in the three previous clusters, which is surprising, because only two hydrogen bonds exist in this conformation compared with three in the previous clusters. The dipole moment (2.06 D) is in the range of those of the other three clusters.

3.3.5. Structures. For all these clusters, the Si−O$_b$ bond linking the chain with the ring is strong: 1.63 Å in the single-branched ring, 1.61−1.64 Å in the *trans*-branched ring, 1.62−1.64 Å in the *cis*-branched ring and 1.61 Å in the double-branched ring. In compensation, the next Si−O$_b$ bond in the chain is much weaker: 1.66−1.67 Å in the *trans*- and *cis*-branched rings and 1.66 Å in the double-branched ring. These bonds are even longer than in the ring: 1.64−1.66 Å for the single-branched ring, 1.64−1.66 Å for the *trans*-branched

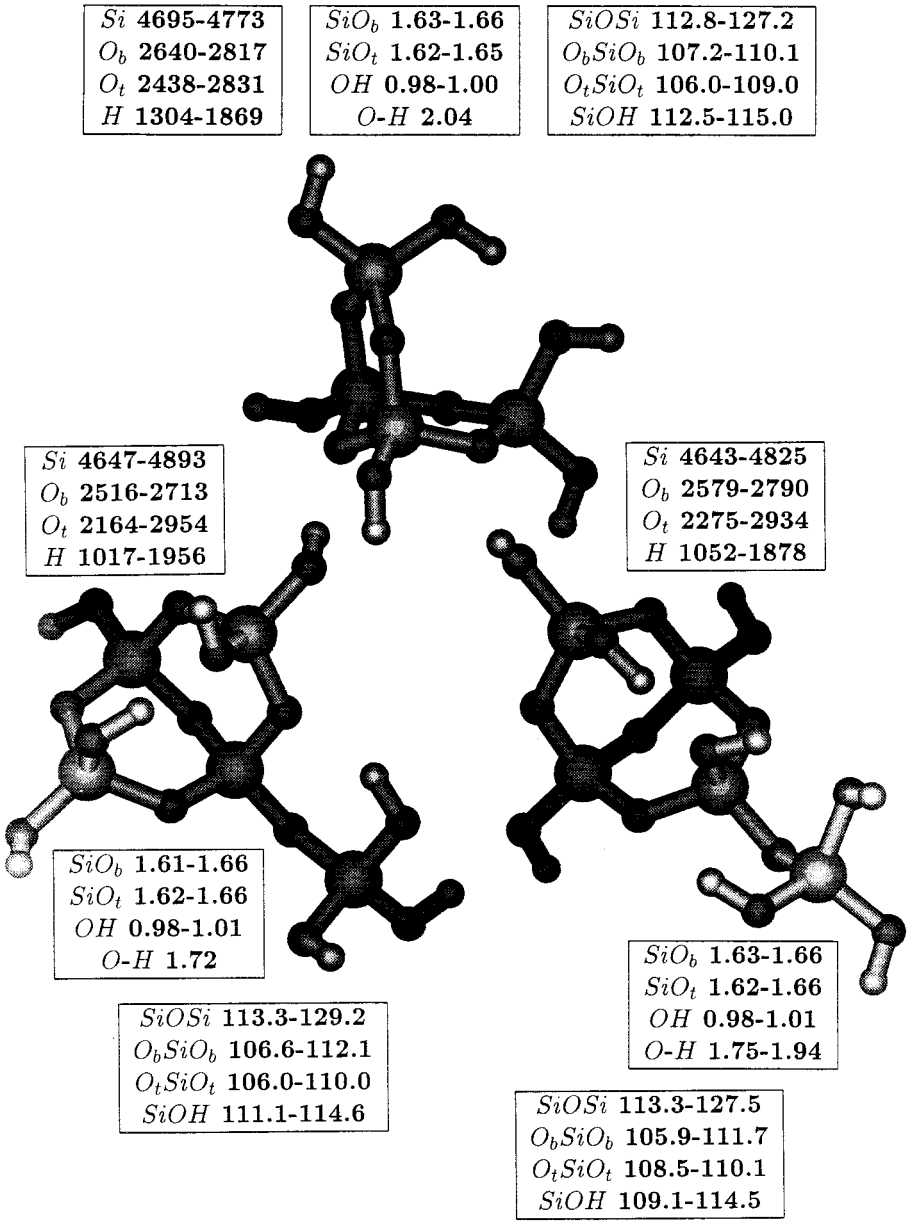

Figure 5. Bond lengths (Å), bond angles (degrees), and Hirshfeld atomic charges (0. and minus signal in O charges are omitted) for $Q_2^3\,Q_2^2$, $Q_2^3\,Q_1^3\,Q_1^2\,Q_1^1$, and $Q_2^2\,Q_1^4\,Q_1^3\,Q_1^1$, optimized at the DF-BHL/DNP level of approximation. Total energy: $E = -1980.0136$ Ha ($Q_2^3\,Q_2^2$), $E = -2494.0106$ Ha ($Q_2^3\,Q_1^3\,Q_1^2\,Q_1^1$) and $E = -2494.0076$ Ha ($Q_2^2\,Q_1^4\,Q_1^3\,Q_1^1$). Dipole moment: $\mu = 2.82$ D ($Q_2^3\,Q_2^2$), $\mu = 2.51$ D ($Q_2^3\,Q_1^3\,Q_1^2\,Q_1^1$) and $\mu = 3.36$ D ($Q_2^2\,Q_1^4\,Q_1^3\,Q_1^1$).

ring, 1.64−1.67 Å for the *cis*-branched ring, and 1.64−1.65 Å for the double-branched ring. This trend was already observed for the one-silicon branched trimer ring.

The other Si−O and OH bond lengths follow the trends observed in previous clusters: 1.63−1.64 Å and 0.98−0.99 Å for unconstrained OH groups, 1.65−1.67 Å and 0.98−0.99 Å for OH donor groups, and 1.62−1.64 Å and 0.99−1.01 Å for acceptors.

The range of variation of the Si−O−Si bond angle is different in the four clusters. In the single-branched ring, the Si−O−Si angle is almost constant in the ring (≈121°), changing slightly more in the chain (117.5−123.7°). In the *trans*-branched ring, the Si−O−Si angles are almost equal in the chains (126.1−130.1°) but change considerably in the ring (115.5−127.8°) owing to the distortions caused by the lateral chains. In the *cis*-branched and double-branched clusters, the Si−O−Si angles are similar: 116.0−124.2° in the chain and 119.2−123.8° in the ring for the *cis*-branched cluster, plus 125.5−133.0° in the chain and 122.8−126.8° in the ring for the double-branched cluster. For all clusters, the Si−O−H angles are similar in terminal hydroxyl groups and in the OH groups forming hydrogen bonds (roughly 111−114°).

3.4. Double Rings: Double Trimer Rings. The double rings, with two intramolecular condensations, are the most strained clusters studied in this work. In this section we analyze briefly the double trimer rings sharing a common edge. In experimental work these clusters are usually not observed.

3.4.1. Double Trimer Ring. The structure and charge distribution for the clusters with two trimer rings bonded by an edge are presented in Figure 5. The four-silicon double ring (above, in the Figure), which is never found in sol−gel solutions,[4,8,10] is the least stable cluster discussed in this work. This is due to the substantial ring strain of the two rings (both with chair conformations), which is increased by the additional constraint of sharing a common Si−O−Si edge. Furthermore, only a single hydrogen bond can be formed, at a reasonable distance of 2.0

Å, because the two rings force the remaining hydroxyl groups to be too far apart to interact with each other.

The condensation energy for this cluster consequently is positive and relatively high (+6.4 kcal mol^{-1}), making its formation very improbable, in agreement with experimental evidence. The dipole moment is quite large (2.82 D), a feature already observed for the trimer ring.

3.4.2. Inner Branched Double Trimer Ring. The inner branched double trimer ring (see Figure 5, below left) results from the association of the four-silicon double ring with a monomer, in such a way that one silicon is bonded to four bridging oxygens. Both rings have chair conformations, very similar to the four-silicon double ring, but more flat than in the three-silicon ring.

There are two hydrogen bonds in this cluster, one between OH groups in different rings (O- -H = 2.02 Å) and another between a bridging oxygen and a OH group in the lateral chain (O- -H = 1.72 Å); the latter appears to be overestimated. The small condensation energy for this cluster (−0.2 kcal mol^{-1}) is again caused by the ring strain, and in fact should be more positive, because of the overestimated hydrogen-bond. The corrected condensation energy of +3.1 kcal mol^{-1} is reasonable, although perhaps slightly too high when compared with the value obtained for the four-silicon double ring (+6.4 kcal mol^{-1}), without the lateral chain and a single hydrogen bond. The dipole moment increases with the addition of the lateral chain, changing from 2.82 D in the double ring to 3.36 D in this branched double ring, perhaps as a result of the separation of the ring from the chain.

3.4.3. Outer Branched Double Trimer Ring. The outer branched double trimer ring (see Figure 5, below right) differs from that discussed above because the monomer is attached to a silicon atom belonging to a single ring, forming a system with two hydrogen bonds, with O- -H distances calculated as 1.94 and 1.75 Å, the latter apparently being too short.

The condensation energy (−2.1 kcal mol^{-1}) is slightly lower than for the previous cluster (−0.2 kcal mol^{-1}), which is as expected, because all silicon atoms are attached to three bridging oxygens at the maximum, whereas in the previous cluster a silicon atom was bonded to four bridging oxygens, thereby increasing the cluster strain. The corrected condensation energy (+1.2 kcal mol^{-1}) is reasonable, given the strain accumulated in the double ring. The electric dipole moment is considerably smaller in this cluster (2.51 D) than in that discussed previously (3.36 D), which is surprising, considering that it is significantly longer (10.4 Å, compared to 8.7 Å in the previous cluster).

3.4.4. Structures. In the four-silicon double ring, the Si−O bond length changes considerably in the constrained rings (1.63−1.66 Å), but is quite short in terminal groups (only 1.62−1.63 Å), increasing, as expected, for groups forming hydrogen bonds (1.65 Å), as the OH bond length (0.99−1.00). Because of the symmetry of the trimer−trimer framework, the Si−O−Si angles are all relatively similar, for the three clusters (≈122−127°), except the Si−O−Si angle in the edge common to both rings, which is much smaller, but again almost constant (≈113°).

In the second cluster, the Si−O distances in the rings are relatively large (1.64−1.68 Å) because of the ring strain, but the first Si−O bond in the lateral chain is very strong: Si−O = 1.61 Å. This bonding effect corroborates the observations made previously for all the trimer branched rings. The Si−O bond lengths in the third cluster also change considerably but are slightly shorter (1.63−1.66 Å) than in the previous cluster, confirming the smaller ring strain and higher stability of the third cluster over the second.

For all three clusters, the Si−OH angles are similar in terminal OH groups (111.7−114.6°) and when constrained by hydrogen bonds (109.1−113.8°). The constrained O_b−Si−O_b and terminal O_t−Si−O_t angles are close to the tetrahedral value.

3.5. Double Rings: Corner-Bonded Double Trimer Ring, Trimer−Tetramer Rings. The trimer−trimer double ring with the two rings bonded by a single silicon is discussed here, together with the two tetramer-trimer rings. Although relatively strained, both tetramer−trimer rings have been found in experimental work and our calculations also suggest that both clusters should be relatively stable.

3.5.1. Corner-Bonded Double Trimer Ring. The structure and charge distribution of the corner-bonded double trimer ring, and of the trimer−tetramer double rings, are shown in Figure 6. In the corner-bonded double trimer ring (right, in the figure), two three-silicon rings are attached to each other by a single silicon atom, instead of an Si−O−Si edge, as in the three clusters discussed previously. The conformation proposed here is particularly favorable because it takes advantage of the chair conformation of both rings to allow the formation of four hydrogen bonds (O- -H = 1.72 Å, 1.86−1.88 and 2.60 Å), that will considerably stabilize this cluster.

The condensation energy of −1.6 kcal mol^{-1} is reasonable, although it could be expected that this cluster would be significantly more stable than the two discussed previously, because of the four hydrogen bonds and because the single corner attachement instead of the shared edge between the two rings should decrease the strain. The corrected energy is already positive, +1.7 kcal mol^{-1}. The dipole moment is particularly high in this cluster, 3.84 D, but the accuracy of the calculation is again questionable and it would be useful to recalculate it with a better level of approximation.

3.5.2. Edge-Bonded Trimer−Tetramer Double Ring. In the edge-bonded trimer−tetramer double ring (see Figure 6, below left), a four-silicon ring and a three-silicon ring share a common Si−O−Si chain, where a hydroxyl group in the three-silicon ring forms two hydrogen bonds with OH groups in the four-silicon ring, increasing even more the rigidity of the cluster. The three-silicon and four-silicon rings keep the usual chair and crown conformations, but the two hydrogen bonds are too short at 1.62−1.63 Å.

The condensation energy obtained for this cluster, of −13.6 kcal mol^{-1}, is probably too negative, even considering that this cluster is found widely in experimental sol−gel solutions. The corrected condensation energy, −7.0 kcal mol^{-1}, is a more acceptable value for a strained double ring structure. The electric dipole moment obtained for this cluster, of 2.54 D, is reasonable, suggesting that the highly symmetrical charge distribution present in the four-silicon ring, whose dipole is only 0.65 D, is not entirely destroyed by the formation of the second ring.

3.5.3. Corner-Bonded Trimer−Tetramer Double Ring. The corner-bonded trimer−tetramer double ring (see Figure 6, above left) differs from the cluster discussed above, because the fragment containing the fifth silicon atom is bonded to two opposite corners of the four-silicon ring, instead of two adjacent ones, as in the cluster before. Owing to this different construction, the crown configuration of the tetramer ring is distorted, although two hydrogen bonds are still formed (O- -H = 1.81−1.82 Å).

The corresponding total condensation energy (−8.6 kcal mol^{-1}) is considerably lower than for the edge-bonded cluster before, because forming the additional chain over the four-silicon ring is energetically less favorable than forming a lateral three-silicon ring. When corrected in the usual way, the energy

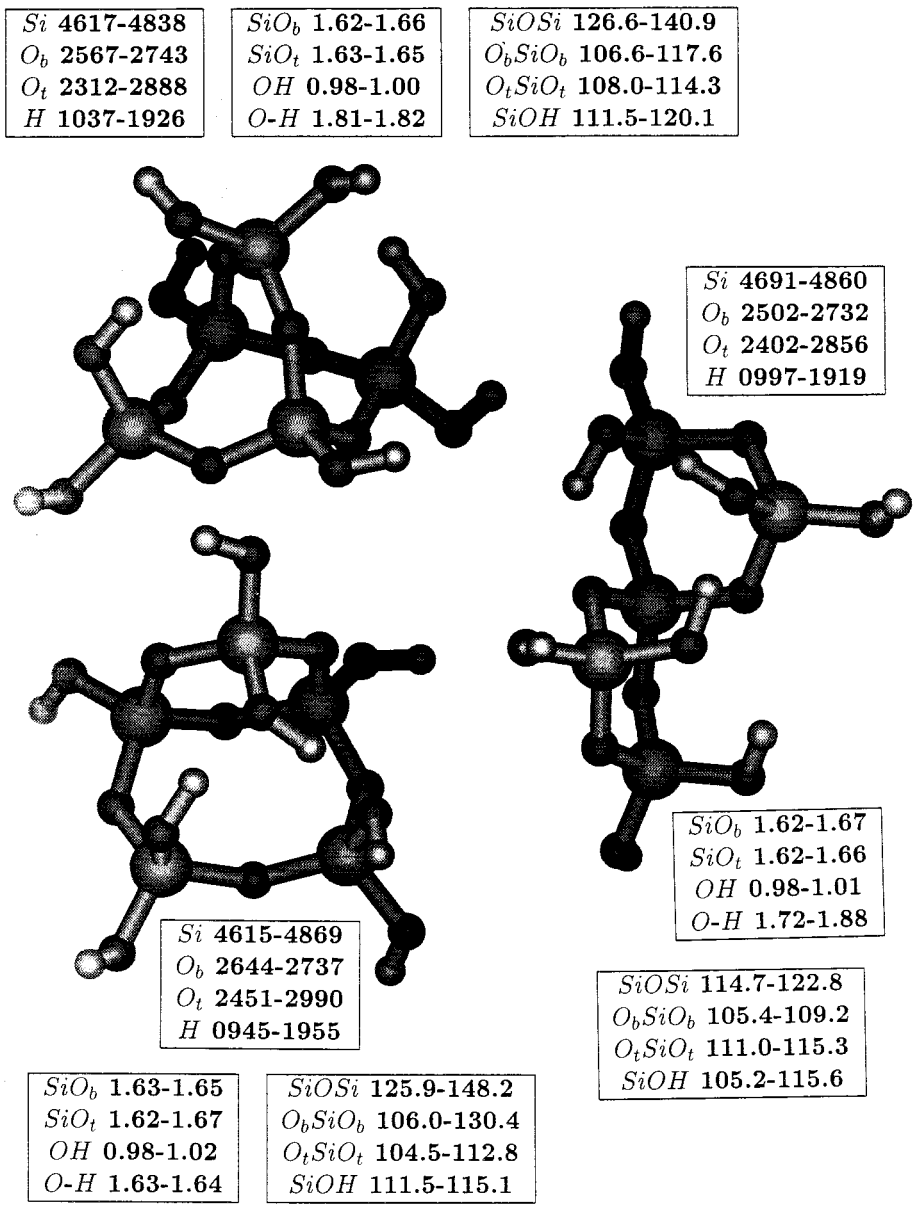

Figure 6. Bond lengths (Å), bond angles (degrees), and Hirshfeld atomic charges (0. and minus signal in O charges are omitted) for $Q_4^2\,Q_1^4$, $Q_2^2\,Q_2^3\,Q_1^2e$ and $Q_2^2Q_2^3Q_1^2c$, optimized at the DF-BHL/DNP level of approximation. Total energy: $E = -2494.0098$ Ha ($Q_4^2\,Q_1^4$), $E = -2494.0289$ Ha ($Q_2^2\,Q_2^3\,Q_1^2e$) and $E = -2494.0209$ Ha ($Q_2^2\,Q_2^3\,Q_1^2c$). Dipole moment: $\mu = 3.84$ D ($Q_4^2\;Q_1^4$), $\mu = 2.54$ D ($Q_2^2\,Q_2^3\,Q_1^2e$) and $\mu = 5.99$ D ($Q_2^2\,Q_2^3\,Q_1^2c$).

is estimated as -2.0 kcal mol^{-1}, which appears to be too positive when compared with the double trimer rings, which have almost the same energy and are observed much less in experimental work.

The strangest feature of this cluster, however, is its extremely high dipole moment (5.99 D), which is very difficult to explain. There may be a lower energy conformation, which would also explain the apparently low stability of this cluster. However, because this is a highly constrained cluster, there are few degrees of freedom and major improvements to the proposed conformation are unlikely.

3.5.4. Structures. In the corner-bonded, trimer−trimer cluster, the Si−O bond lengths change considerably in the double ring framework (1.62−1.67 Å), essentially because the different chemical environment of the central and the outer silicon atoms. The Si−O and OH bond distances in the hydroxyl groups are similar to those in the previous clusters.

The Si−O−Si angle has a surprisingly small range of variation (114.7−122.8°), considering that this is a highly strained cluster, where the central silicon atom (bonded to four bridging oxygens) has a different environment from the other four (bonded to only two bridging oxygens). The O_b-Si-O_b angle is ≈5° larger than the O_t-Si-O_t angle.

In the edge-bonded tetramer−trimer ring, because the hydrogen bonds are so strong, the Si−O and OH distances in hydroxyl groups have a significant range of variation: 1.62−1.67 Å and 0.98−1.02 Å, respectively. The OH length in the acceptors (1.02 Å) and the Si−O length in the donors (1.67 Å) appears to be too long, whereas the Si−O distance in the acceptors (1.62 Å) is probably too short, resulting from the LDA level of approximation. The bridging $Si-O_b$ bond length also changes considerably (1.62−1.65 Å) because of the three different silicon environments (Q_2^3, Q_2^2 and Q_1^2) in the edge-bonded cluster.

In the corner-bonded tetramer−trimer ring, the Si−O and OH distances in the hydroxyl groups (1.63−1.65 Å and 0.98−1.0 Å) change less than in the edge-bonded cluster before. Each bridging oxygen forms a shorter bond (1.62−1.63 Å) and a

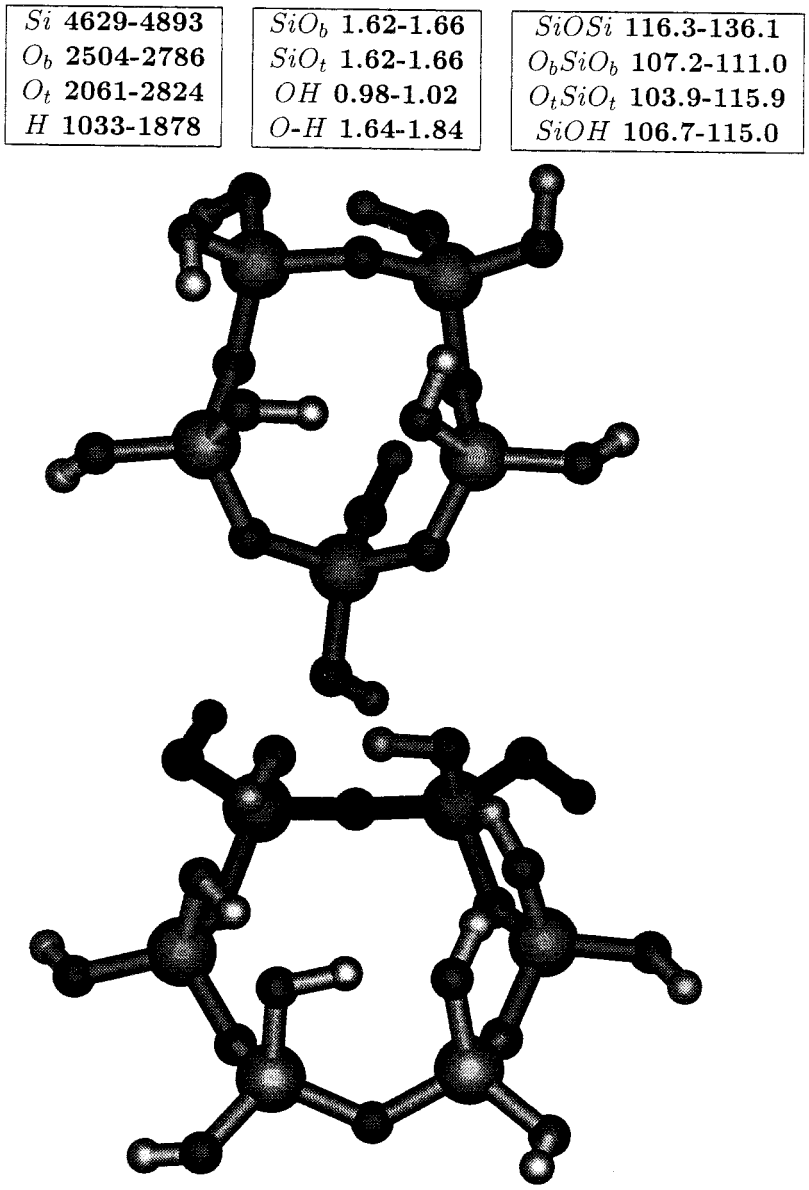

Figure 7. Bond lengths (Å), bond angles (degrees), and Hirshfeld atomic charges (0. and minus signal in O charges are omitted) for large rings, optimized at the DF-BHL/DNP level of approximation. Total energy: $E = -2569.9577$ Ha (Q_5^2) and $E = -3083.9788$ Ha (Q_6^2). Dipole moment: $\mu = 3.39$ D (Q_5^2) and $\mu = 0.82$ D (Q_6^2).

longer one (1.65−1.66 Å). The Q_2^3 silicons belonging to both rings have two short and one long Si−O_b bond lengths, whereas the other Q_2^2 bridging silicons have two long bonds and the fifth Q_1^2 silicon two short ones.

Because of the ring structure, the Si−O−Si angles change considerably in the corner-bonded tetramer−trimer ring, becoming smaller in the four-silicon ring (126.6−135.5°) than in the upper chain (see Figure 6) formed by the fifth silicon atom (136.3−140.9°). In the edge-bonded tetramer−trimer ring, the Si−O−Si bond angle is larger (148.2°) in the more relaxed tetramer ring edge opposite to the trimer ring than in the other cyclic bonds (125.9−130.4°).

In the edge-bonded tetramer−trimer ring, the Si−O−H angles change little (112−115°), but in the corner-bonded ring, when hydrogen bonds are present, the Si−OH angles have larger values than usual (as large as 120°). The O_b−Si−O_b angles also change considerably in this cluster (106.6−117.6°), which is surprising for such a hard angle.

3.6. Larger Rings: Five- and Six-Silicon Rings. Finally we analyze the larger five- and six-silicon rings. Our results suggest that, in vacuo, the four- and six-silicon rings are stabilized more by strong hydrogen-bond systems than the five-silicon cluster, which lacks the required symmetry.

3.6.1. Five-Silicon Ring. The structure and charge distribution for the five- and six-silicon rings are presented in Figure 7. The five-silicon ring has the S shape conformation usually proposed for ten-carbon rings (see ref 11). The S shape is distorted, however, by four hydrogen bonds present in this conformation

(O- -H = 1.64 Å, 1.84, 1.98, and 2.01 Å); the first two are probably overestimated.

The total condensation energy for the five-silicon ring (above, in the Figure) is smaller (−25.1 kcal mol^{-1}) than for the four-silicon ring (−25.7 kcal mol^{-1}), because the symmetry is much smaller, and a cyclic hydrogen-bond system is no longer present. However, the LDA corrected energy (−18.5 kcal mol^{-1}) is already lower than the value obtained for the tetramer ring (−12.5 kcal mol^{-1}). The larger five-silicon ring allows a better relaxation of the ring strain, although stronger hydrogen bonds may be formed in the four-silicon ring, where the hydroxyl groups are closer to each other. The dipole moment in the five-silicon ring is quite large (3.39 D), particularly when compared with the four-silicon ring (0.65 D), owing to its poor symmetry, due to the distortion caused by the hydrogen bonds.

3.6.2. Six-Silicon Ring. The six-silicon ring (see Figure 7, below) has an "extended crown" conformation, with six hydroxyl groups forming a cyclic hydrogen bond system, which greatly stabilizes the cluster. These hydrogen bonds are seriously overestimated, because the O- -H bond lengths (1.56−1.60 Å) are too short, and the corresponding O−H bond lengths (1.03−1.04 Å) are too large. Consequently, the total condensation energy for the six-silicon ring (−48.7 kcal mol^{-1}) is likely to be overestimated. The corrected value (−28.9 kcal mol^{-1}) is a much more sensible value.

The dipole moment of the six-silicon ring is much smaller (0.88 D) than for the three- and five-silicon rings, although slightly larger than in the tetramer ring. At the LDA level of approximation, the "chair" conformation of the trimer ring produces a much larger charge separation than the "crown" or "extended crown" conformations proposed for the four- and six-silicon rings.

3.6.3 Structures. The hydrogen bond distortions in the five-silicon ring explain the large bond length variations in bridging (Si−O_b = 1.62−1.66 Å) and terminal groups (Si−O_t = 1.62−1.64 Å and OH = 0.98−1.02 Å). In the six-silicon ring, the terminal groups in equatorial positions have normal OH lengths (0.98 Å), but the Si−O bonds are much stronger (1.63 Å) than in the hydrogen bond system (1.65−1.66 Å). In the five-silicon ring, the O_b−Si−O_b bond angles change very little, but the Si−O−Si (116.3−136.1°) and O_t−Si−O_t (103.9−115.9°) bond angles vary considerably, because of the hydrogen bonds. The Si−OH angles are almost constant in terminal OH groups (113.3−115.0°), again changing more when constrained by hydrogen bonds (106.7−112.0°).

In the six-silicon ring, the Si−O−H angles are also smaller in the hydrogen bond system (106.4−108.1°) than in the terminal OH groups (111.9−115.3°). The Si−O−Si angles (127.1−130.0°) are relatively similar to those in the four-silicon ring, although much larger than in the trimer ring.

4. Discussion

The predicted structural data (bond lengths and bond angles), charge distribution (electric dipole moments and Hirshfeld charges), and total condensation energies (calculated and corrected energies, divided by the number of condensation reactions, and by the number of silicon atoms), for all silica clusters studied in this work, are presented in Tables 1, 2, 3, and 4.

As discussed in the previous paper, the LDA method tends to overestimate the condensation energies of the silica clusters, as shown by the total condensation energy for the smallest clusters: for the dimer, −9.4 kcal mol^{-1} (DF-BHL/DNP), −2.8 kcal mol^{-1} (DF-BLYP/DNP), and −2.2 kcal mol^{-1} (DF-BLYP/TNP); for the linear trimer, −18.5 kcal mol^{-1} (DF-BHL/DNP) and −7.7 kcal mol^{-1} (DF-BLYP/DNP); and for the cyclic trimer, −1.6 kcal mol^{-1}) (DF-BHL/DNP) and +5.5 kcal mol^{-1} (DF-BLYP/DNP). Consequently, the total condensation energies obtained in this work, at the DF−BHL/DNP level, for example for the linear tetramer (−38.2 kcal mol^{-1}), the tetramer ring (−25.7 kcal mol^{-1}), the linear pentamer (−43.6 kcal mol^{-1}), and the six-silicon ring (−48.7 kcal mol^{-1}), are likely to decrease considerably when recalculated with nonlocal density (and a better basis set).

Because the condensation energies calculated for the dimer with a double numerical basis set (−2.8 kcal mol^{-1}) and a triple numerical basis set (−2.2 kcal mol^{-1}) are similar, the LDA energies were corrected to fit the values for the dimer obtained with a double instead of a triple basis set, to correct exclusively the nonlocal effects necessary to describe hydrogen bonds accurately. However, even the corrected energies are still more negative than the DF-BLYP/DNP values, as shown by the linear trimer (corrected BHL, −11.9 kcal mol^{-1}; BLYP, −7.7 kcal mol^{-1}) and trimer ring (corrected BHL, −1.6 kcal mol^{-1}; BLYP, +5.5 kcal mol^{-1}). This might be due to the chosen criterion of correcting only the hydrogen bonds that were more obviously overestimated, with O−H distances smaller than 1.85 Å. The corrected energies will be used in almost all the discussion that follows.

The total condensation energy, to form a silica cluster from the monomer (in the gas phase) depends essentially on its structure (hydrogen bonds, number and type of rings) and size. Table 4 shows the calculated (and corrected) condensation energies for all clusters, divided by the number of silicon atoms, and by the number of condensation reactions necessary to create them, which we denote the intrinsic condensation energy.

This intrinsic energy is small for the dimer (−2.8 kcal mol^{-1}) but increases considerably for the linear trimer (−6.0 kcal mol^{-1}), and then slowly for the linear tetramer (−7.2 kcal mol^{-1}) and the linear pentamer (−7.6 kcal mol^{-1}). Probably the value for the dimer is small because the hydrogen bonds tend to decrease the O- -H distances and consequently the Si−O−Si angle also, an energetically unfavorable change. It is possible thus to predict a total condensation energy for the six-silicon linear chain (for example) of approximately −39.0 kcal mol^{-1} (−7.8 kcal mol^{-1} per condensation reaction). This variation is similar for the straight conformations (uncorrected because the O−H distances are longer than 1.85 Å): trimer (−7.8 kcal mol^{-1}), tetramer (−8.9 kcal mol^{-1}), and pentamer (−8.1 kcal mol^{-1}).

The intrinsic condensation energies for the rings show also a predictable evolution: trimer ring (−0.5 kcal mol^{-1}), tetramer ring (−3.1 kcal mol^{-1}), pentamer ring (−3.7 kcal mol^{-1}), and six-silicon ring (−4.8 kcal mol^{-1}). These energies are less negative than for the linear chains, becoming more and more negative as the ring becomes larger and more relaxed. At the corrected LDA level of approximation, it is thus possible to predict a condensation energy for the seven-silicon ring, for example, of ≈ −36.4 kcal mol^{-1} (corresponding to an intrinsic energy per reaction of −5.2 kcal mol^{-1}). For progressively larger rings, the intrinsic energy should converge to the value for linear chains (about −7.8 kcal mol^{-1}).

Linear clusters are more stable than branched ones, although the differences are small, as the intrinsic condensation energies show: linear pentamer (−7.6 kcal mol^{-1}), branched pentamer (−6.8 kcal mol^{-1}), and pentamer cross (−5.5 kcal mol^{-1}). The same is calculated for the four-silicon clusters, before the energies are corrected: the energy of the linear chain is about

7.5 kcal mol^{-1} lower than the branched one. The order changes, however, after correcting the energies, because the intrinsic energies are calculated as -7.2 kcal mol^{-1} for the linear tetramer and -8.0 kcal mol^{-1} for the branched tetramer.

Introducing a lateral chain in a ring decreases the intrinsic condensation energy by about 0.5−1.0 kcal mol^{-1}: branched trimer ring (-1.5 kcal mol^{-1}) compared with the trimer ring (-0.5 kcal mol^{-1}); branched tetramer ring (-3.6 kcal mol^{-1}) compared with the tetramer ring (-3.1 kcal mol^{-1}); branched double trimer rings (-0.2 and $+0.5$ kcal mol^{-1}) compared with the double ring ($+1.3$ kcal mol^{-1}). The five-silicon clusters with a trimer ring have essentially the same energy: -1.4 kcal mol^{-1} for the ring with two *cis* chains and -2.2 kcal mol^{-1} for the rings with two *trans* chains, a two silicon chain, and two chains attached to the same silicon. The position of the chains in the trimer ring is therefore not important for the energies of these reactions, but this factor may change for larger rings. For example, the ortho-branched tetramer ring might have a lower energy than its meta isomer, where hydrogen bonds between the two lateral chains are not possible.

The three five-silicon clusters with two trimer rings have also very similar condensation energies: $+0.5$ kcal mol^{-1} for the edge-bonded double ring with a Q_1^4 silicon; -0.2 kcal mol^{-1} for the edge-bonded double ring with three Q_3^3 silicons and $+0.3$ kcal mol^{-1} for the corner-bonded double ring. In this case, the condensation energy is almost independent of the kind of attachement of the two rings and of the position of the lateral chain. The intrinsic condensation energy also changes very little from the three-silicon ring (-0.5 kcal mol^{-1}), to the four-silicon edge bonded double ring ($+1.3$ kcal mol^{-1}), and the five-silicon corner-bonded double ring (-0.3 kcal mol^{-1}).

It is also worthwhile to compare the three pentamers with a tetramer ring: as expected, the condensation energy is significantly lower (-3.6 kcal mol^{-1}) when the fifth silicon forms just a lateral chain than when a further intramolecular condensation leads to the formation of a edge-bonded trimer ring (-1.2 kcal mol^{-1}). When the fifth silicon fragment is bonded to opposite corners of the tetramer ring, straining even further the cluster and actually creating two additional four-silicon rings, the energy increases again (to only -0.3 kcal mol^{-1}). Nevertheless, these energies are still similar, given the different structures of the clusters; the open and closed trimer energies, for example, change much more, from -6.0 kcal mol^{-1} to -0.5 kcal mol^{-1}.

As expected, the energy difference (-1.5 kcal mol^{-1}) between the strained branched trimer ring and the tetramer ring (-3.1 kcal mol^{-1}) is still significant, but the more relaxed branched tetramer ring (-3.6 kcal mol^{-1}) and the five-silicon ring (-3.7 kcal mol^{-1}) have virtually the same energy. Finally, the corrected energies obtained for the various clusters are much more consistent with the energy obtained for the cubic octamer ($+0.3$ kcal mol^{-1}), the only cluster (apart from the monomer) where hydrogen bonds are not present and consequently where the LDA approximation should work well, without any need for a correction.

5. Conclusions

To understand the complex mechanisms of reaction, solvation, and diffusion that determine the chemistry of silica in solution, it is necessary to study first the silicate clusters that participate in these processes. This study reveals a wide diversity of structures and consequently of charge distributions and energies for these clusters, that influences directly their chemical behavior, particularly their interaction with other clusters and with the solvent.

The results presented here show that the stability of the noncyclic clusters decreases with the degree of branching, as observed experimentally. This trend is observed for both four-silicon and five-silicon clusters. All branched cyclic clusters have the ring conformation of the corresponding unbranched rings, which occurs despite the hydrogen bonds formed between the chains and the ring that could force a rearrangement of the cyclic frame. The Si−O bond which links the ring with the lateral chain is much stronger than the equivalent bonds in the ring and in the chain.

As expected, the double ring clusters are quite unstable, particularly the double trimer rings, corner-linked and edge-linked, which have essentially the same energy. The trimer−tetramer rings are easier to form, particularly the edge-linked structure.

The four- and six-silicon rings are more stable than the five-silicon ring because of the relatively asymmetric arrangement of the latter. However, the small trimer ring, despite its internal strain and low stability has a highly symmetric optimized structure.

The information thus acquired with the systematic analysis of the smallest silica clusters can be used to construct a kinetic model suitable to describe the first steps of silica growth, as reported in a later paper. Studies with higher accuracies and simulating a liquid environment will be reported in future publications.

Acknowledgment. We are grateful to EPSRC for funding the local and national computer facilities used for this work. One of the authors (J.C.G.P.) is greatly indebted to Instituto Superior Técnico, Department Eng. Materiais, Lisboa, and JNICT, Programa Ciência and programa Praxis XXI, Lisboa, for their financial support. We would like to thank MSI for provision of software.

References and Notes

(1) Pereira, J. C. G.; Catlow, C. R. A.; Price, G. D. *J. Phys. Chem.* **1999**, *00*, 0000.
(2) Iler, R. K. *The Chemistry of Silica*, John Wiley & Sons: New York, 1979.
(3) Brinker, C. J.; Scherer G. W. *Sol−Gel Science: The Physics and Chemistry of Sol−Gel Processing*; Academic Press: New York, 1989.
(4) Kelts, L. W.; Amstrong, N. J. *J. Mater. Res.* **1989**, *4*, 2, 423.
(5) Klemperer, W. G.; Mainz, V. V.; Millar, D. M. In *Better Ceramics Through Chemistry II*; Brinker, C. J.; Clark, D. E.; Ulrich, D. R., Eds.; Materials Research Society, Vol. 73; Elsevier: New York, **1986**; p 3.
(6) Klemperer, W. G.; Mainz, V. V.; Millar, D. M. In *Better Ceramics Through Chemistry II*; Brinker, C. J.; Clark, D. E.; Ulrich, D. R., Eds.; Materials Research Society, Vol. 73; Elsevier: New York, **1986**; p 15.
(7) Klemperer, W. G.; Ramamurthi, S. D. In *Better Ceramics Through Chemistry III*; Brinker, C. J.; Clark, D. E.; Ulrich, D. R., Eds.; Materials Research Society, Vol. 121; Elsevier: New York, **1988**; p 1.
(8) Klemperer, W. G.; Mainz, V. V.; Ramamurthi, S. D.; Rosenberg, F. S. In *Better Ceramics Through Chemistry III*; Brinker, C. J.; Clark, D. E.; Ulrich, D. R., Eds.; Materials Research Society, Vol. 121; Elsevier: New York, **1988**; p 15.
(9) Klemperer, W. G.; Ramamurthi, S. D. In *J. Non-Cryst. Solids* **1990**, *121*, 16.
(10) Knight, C. T. G. *Zeolites* **1990**, *10*, 140.
(11) Dunitz, J. D.; Ibers, J. A. *Perspectives in Structural Chemistry II*; John Wiley & Sons: New York, 1968.
(12) Galeener, F. L. *J. Non-Cryst. Solids* **1982**, *49*, 53.
(13) Hill, J.; Sauer, J. *J. Chem. Phys.* **1994**, *98*, 1238.
(14) Moravetski, V.; Hill, J.; Eichler, U.; Cheetham, A. K.; Sauer, J. *J. Am. Chem. Soc.* **1996**, *118*, 13015.
(15) West, J. K.; Zhu, B. F.; Cheng, Y. C.; Hench, L. L. *J. Non-Cryst. Solids* **1990**, *121*, 51.
(16) West, J. K.; Wallace, S.; Hench, L. L.; Lishawa, C. R. In *Ultrastructure Processing of Advanced Materials*; Uhlmann, D. R.; Ulrich, D. R., Eds.; John Wiley & Sons: New York, 1992, chapter 11.
(17) Lasaga, A. C.; Gibbs, G. V. *Phys. Chem. Miner.* **1987**, *14*, 107.
(18) Lasaga, A. C.; Gibbs, G. V. *Phys. Chem. Miner.* **1988**, *16*, 29.

(19) Pápai, I.; Goursot, A.; Fajula, F. *J. Chem. Phys.* **1994**, *98*, 4654.
(20) Garofalini, S. H.; Martin, G. *J. Phys. Chem.* **1994**, *98*, 1311.
(21) Feuston, B. P.; Garofalini, S. H. *J. Phys. Chem.* **1990**, *94*, 5351.
(22) Feuston, B. P.; Garofalini, S. H. *J. Chem. Phys.* **1988**, *89*, 9, 5818.
(23) Catlow, C. R. A.; Coombes, D. S.; Lewis, D. W.; Pereira, J. C. G. *Chem. Mater*. **1998**, *10*, 3249.
(24) *Dmol 96.0 Manual*; Molecular Simulations: San Diego, CA, 1996.
(25) von Barth, U.; Hedin L. *J. Phys. C: Solid State Phys.* **1972**, *5*, 1629.
(26) Hedin, L.; Lundqvist B. I. *J. Phys. C: Solid State Phys.* **1971**, *4*, 2064.
(27) Moruzzi V. L.; Janak J. F.; Schwarz K. *Phys. Rev. B* **1988**, *37*, 2, 790.
(28) Delley, B. *Chem. Phys.* **1986**, *110*, 329.
(29) Kubicki, J. D.; Lasaga A. C. *Am. Miner*. **1988**, *73*, 941.
(30) Sauer, J. *Chem. Rev.* **1989**, *89*, 199.
(31) Mozzi, R. L.; Warren B. E. *J. Appl. Crystallogr*. **1969**, *2*, 164.